Pergamon

S0360-5442(96)00008-4

Energy Vol. 21, No. 6, pp. 435–443, 1996

0360-5442/96 $15.00 + 0.00

EFFICIENCY IMPROVEMENT OF FLAT-PLATE SOLAR AIR HEATERS

HO-MING YEH† and TONG-TSHIEN LIN

Department of Chemical Engineering, Tamkang University, Tamsui, Taiwan, R.O.C.

(Received 2 November 1995)

Abstract—The effect of parallel barriers on the collector efficiency of flat-plate solar air heaters has been investigated theoretically and experimentally. The barriers were placed with uniform spacing and in parallel, thereby dividing the air channel (collector) into parallel subchannels (subcollectors) of the same size. These subcollectors were connected in series so that air flowed through them in sequentially reversed directions. Experimental studies were performed for different locations of the barriers. The theoretical predictions agree reasonably well with experimental results. The optimal barrier location for maximum collector efficiency is the center line of the collector. The collector efficiency increases theoretically as the number of barriers increases.

INTRODUCTION

Flat-plate solar collectors are designed for applications requiring energy delivery at moderate temperatures. They utilize both beam and diffuse solar radiation, and do not require sun tracking. The solar air heater occupies an important place among solar heating systems because of minimal use of materials. Furthermore, the direct use of air as the working substance reduces the number of required system components. The primary disadvantage of solar air heaters is the need for handling relatively large volumes of air with low thermal capacity as working fluid. The primary applications are space heating and drying.

Our design of a solar air heater has an extended heat-transfer area,[1] arrangements for producing free convection[2,3] and creation of air turbulence behind the heating surface,[4] as well as inclusion of strong forced convection. It is well known that the collector configuration was influence the fluid velocity and also the strength of forced convection. A simple procedure for changing the fluid velocity and the strength of forced convection involves adjusting the aspect ratio of a rectangular, flat-plate collector with constant flow rate.[5] The strength of forced convection may also be enhanced by placing parallel barriers on the flat-plate collector, thereby dividing the collector into several subcollectors.

THERMAL PERFORMANCE OF SUBCOLLECTOR 1

Figure 1 shows the flows in the flat-plate, solar air heater with a barrier on the collector. In Fig. 1, the flow channel (collector) is divided by a barrier into two subchannels (subcollectors) 1 and 2 of different sizes. The air inlet temperature is T_i. Air is first introduced into subcollector 1 where it is preheated. The preheated air flowing out from subcollector 1 at temperature $T_{1,L}$ is then conducted into subcollector 2 for further heating to the outlet temperature T_0.

Collector efficiency

A convenient representation of collector efficiency for subcollector 1 is:

$$\eta_1 = Q_{u,1}/A_{c,1}I_0 = F_{R,1}[\alpha_p\tau_g - U_{L,1}(T_i - T_a)/I_0], \tag{1}$$

in which the heat-removal factor is defined as:

†To whom all correspondence should be addressed.

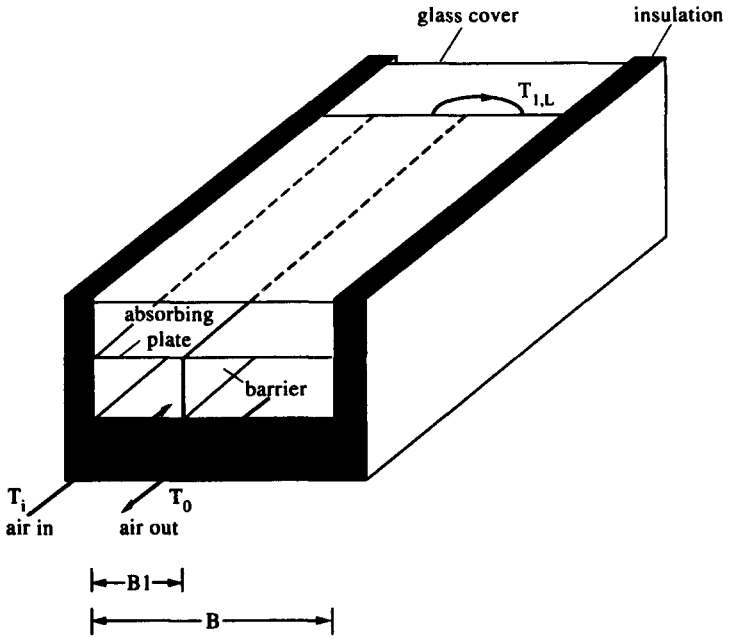

Fig. 1. Flat-plate solar air heater with a parallel barrier.

$$F_{R,1} = (\dot{m}C_p/A_{c,1}U_{L,1})\{1 - \exp[-(U_{L,1}F'_1A_{c,1}/\dot{m}C_p)]\}. \tag{2}$$

Equation (1) was derived from energy balances for sheet-and-tube solar energy collectors[6–8] under the following assumptions: the temperatures of the absorbing plate and bulk fluid are mainly functions of the flow direction and the radiant energies absorbed by the glass cover and fluid are negligibly small.

Although there are many different designs of flat-plate collectors available, it is fortunately not necessary to develop a new analysis for each situation.[7–9] The generalized relations given in Eqs. (1) and (2), which were developed for the tube-and-sheet case, apply to most collector designs. It is only necessary to derive the appropriate form of the collector efficiency factor F′ and Eqs. (1) and (2) may then be used to predict the thermal performance.

The collector-efficiency factor for subcollector 1 is:[10]

$$F'_1 = \{1 + U_{L,1}/h_1 + [(1/h_1) + (1/h_{r,1})]^{-1}\}^{-1}, \tag{3}$$

in which the collector overall-loss coefficient $U_{L,1}$ is the sum of the top ($U_{t,1}$) and bottom and edge (U_b) loss coefficients, i.e.

$$U_{L,1} = U_{t,1} + U_b. \tag{4}$$

Heat-transfer coefficients

The resistance to energy loss through the bottom and edges of the collector results mainly from the resistance to heat flow through the insulation by conduction, i.e.

$$U_b = k_s/l_s. \tag{5}$$

An empirical equation for $U_{i,1}$ was developed by Klein[11] following the basic procedure of Hottel and Woetz.[12] For the horizontal collector shown in Fig. 1

$$U_{t,1} = \left\{ \frac{(T_{p,1}/520)}{\left[\dfrac{(T_{p,1}-T_a)}{1+(1+0.089h_w-0.1166h_w\epsilon_p)(1+0.07866)}\right]^{0.43(1-100/T_{p,1})}} + \frac{1}{h_w} \right\}^{-1}$$

$$+\frac{\sigma(\bar{T}_{p,1}+T_a)(\bar{T}_{p,1}^2+T_a^2)}{(\epsilon_p+0.00591h_w)^{-1}+[2+(1+0.089h_w-0.1166h_w\epsilon_p)(1+0.07866)-1+0.133\epsilon_p]/\epsilon_g-1}. \quad (6)$$

The heat-transfer coefficients between air and two of the duct walls (absorbing and bottom plates) were assumed to be equal to Eq. (3). In the study of solar air heaters and collector-storage walls, it is necessary to know the forced convection heat-transfer coefficient between two flat plates. For air, the following correlation[13] may be derived from Kay's data for fully developed turbulent flow with one side heated and the other side insulated:

$$N_{u,1} = hD_{e,1}/k = 0.0158\mathrm{Re}_1^{0.8}. \quad (7)$$

The characteristic length is the equivalent diameter of the duct, i.e.

$$D_{e,1} = 4HB_1/2(B_1+H) = 2H(B_1/B)/[(B_1/B)+(H/B)]; \quad (8)$$

the Reynolds number for the rectangular duct is then defined by:

$$\mathrm{Re}_1 = D_{e,1}v\rho/\mu = \frac{[4HB_1/(2B_1+2H)][\dot{m}/(\rho B_1H)]\rho}{\mu} = \frac{2\dot{m}/B}{\mu(B_1/B+H/B)}. \quad (9)$$

The radiation coefficient between the two air-duct surfaces may be estimated by assuming a mean radiant temperature equal to the mean fluid temperature, viz.,

$$h_{r,1} \approx 4\sigma\bar{T}_1^3/[(1/\epsilon_p)+(1/\epsilon_R)-1]. \quad (10)$$

The convective heat-transfer coefficient h_w for air flowing over the outside surface of the glass cover depends primarily on the wind velocity V. McAdams[14] obtained the experimental result

$$h_w = 5.7 + 3.8V, \quad (11)$$

where the units of h_w and V are W/m^2–K and m/s, respectively. If the unit of h_w is changed to kJ/h–m^2–K, Eq. (i1) becomes

$$h_w = 4.9 + 3.27V. \quad (12)$$

Mean temperatures

The temperature distribution of the air in subcollector one along the flow direction of the rectangular duct may be obtained from the energy balances in the form:[15]

$$\frac{T_1(z)-T_a-I_0\tau_g\alpha_p/U_{L,1}}{T_i-T_a-I_0\tau_g\alpha_p/U_{L,1}} = \exp\left[-\frac{A_{c,1}F_1'U_{L,1}(z/L)}{\dot{m}C_p}\right]. \quad (13)$$

The mean fluid temperature is then found by integrating Eq. (13) from $z = 0$ to $z = L$, viz.,

$$\bar{T}_1 = (1/L)\int_0^L T_1(z)\mathrm{d}z. \quad (14)$$

Performing this integration and substituting η_1 and $F_{R,1}$ from Eqs. (1) and (2), respectively, the mean fluid temperature is obtained as:

$$\bar{T}_1 = T_i+(\eta_1I_0/U_{L,1}F_{R,1})[[1-(F_{R,1}/F_1')]. \quad (15)$$

This is also the proper temperature for evaluation of fluid properties in subcollector one. The fluid

temperature at the outlet of subcollector one, $T_{1,L}$, is the fluid temperature at the inlet of subcollector two. $T_{1,L}$ may be obtained either by substituting $z = L$ into Eq. (13) to obtain:

$$\frac{T_{1,L}-T_a-I_0\tau_g\alpha_p/U_{L,1}}{T_i-T_a-I_0\tau_g\alpha_p/U_{L,1}} = \exp\left[-\frac{A_{c,1}F_1'U_{L,1}}{\dot{m}C_p}\right], \tag{16}$$

or by taking an energy balance around subcollector one to derive:

$$T_{1,L} = T_i+Q_{u,1}/(\dot{m}C_p). \tag{17}$$

The mean plate temperature will always be greater than the mean fluid temperature due to heat-transfer resistance between the absorbing surface and fluid. The mean plate temperature may be used to calculate the collector efficiency, i.e.

$$\eta_1 = \tau_g\alpha_p-U_{L,1}(\bar{T}_{p,1}-T_a)/I_0. \tag{18}$$

If we equate the relations for η_1 given in Eqs. (18) and (1) and solve for the mean plate temperature, we find:

$$\bar{T}_{p,1} = T_i+(\eta_1 I_0/U_{L,1}F_{R,1})(1-F_{R,1}). \tag{19}$$

Calculation method for collector efficiency

The procedure for calculation of theoretical values of η_1 will now be described. First, with known collector geometries (L, B, B_1, H) and system properties (τ_g, α, C_p, ρ, μ, k, k_s, l_s, ϵ_p, ϵ_R, ϵ_g), as well as the given operating condition (I_0, T_a, V, $\dot{m}$, T_i), a temporary value of η_1 is estimated from Eqs. (1) through (12) once $\bar{T}_{p,1}$ an $\bar{T}_1$ are specified. The values of $\bar{T}_1$ and $\bar{T}_{p,1}$ are then checked by using Eqs. (15) and (19), respectively, and new values of $\bar{T}_1$ and $\bar{T}_{p,1}$ may be obtained. If the calculated values of $\bar{T}_1$ and $\bar{T}_{p,1}$ are different from the assumed values, continued calculations by iteration are needed until the last assumed values meet the finally calculated values. In this manner, the corresponding final value for η_1 is also obtained.

THERMAL PERFORMANCE OF SUBCOLLECTOR 2

The equations and procedure for calculation of the collector efficiency η_2 in subcollector two are the same as those for subcollector one, except that quantities with subscript 1 are replaced by quantities with subscript 2, and that T_i and z are replaced by $T_{1,L}$ and L-z, respectively. $T_{1,L}$ is the air temperature at the outlet of subcollector one and is also the air temperature at the inlet to subcollector two. $T_{1,L}$ may be calculated either from Eq. (16) or (17). It should be noted that $B_2 = B-B_1$ and the total width of the collector B is considered to be constant. As noted previously, the widths of the subcollectors B_1 and B_2 will be changed for both the theoretical predictions and experimental work. The effects of changing B_1 and B_2 on total collector efficiency will also be investigated.

THE TOTAL COLLECTOR EFFICIENCY

The total collector efficiency is defined as:

$$\eta = Q_u/I_0A_c = (Q_{u,1}+Q_{u,2})/I_0(A_{c,1}+A_{c,2}), \tag{20}$$

while the collector efficiencies for subcollectors one and two may be written, respectively, as:

$$\eta_1 = Q_{u,1}/(I_0A_{c,1}), \tag{21}$$

$$\eta_2 = Q_{u,2}/(I_0A_{c,2}) \tag{22}$$

in view of Eq. (1). Equation (20) then becomes:

$$\eta = (\eta_1 A_{c,1} + \eta_2 A_{c,2})/A_c = \eta_1(B_1/B) + \eta_2[1-(B_1/B)], \tag{23}$$

where:

$$A_c = A_{c,1} + A_{c,2} = B_1 L + B_2 L = BL. \tag{24}$$

Thus, after η_1 and η_2 have been calculated for each value of B_1/B as specified in the previous sections, η is readily obtained from Eq. (23).

EXPERIMENTAL STUDIES

Apparatus and procedure. Nine solar air heaters with the same total collector surface area A_c of 0.42135 m^2 (L = 26.5 cm, B = 159 cm) but with different barrier locations (B_1/B) were built. The (B_1/B) ratios were 1/6, 1/5, 1/4, 1/3, 1/2, 2/3, 3/4, 4/5 and 5/6. The barrier used to divide the flow channel into two subchannels was a thin, thermally insulated plate made of asbestos. It is assumed that the two subcollectors are thermally separated. The two subcollectors are connected at one end as shown in Fig. 1. Another solar air heater of the same size but without a barrier ($B_1/B = 1$) was also built for comparison.

In order to maintain steady climatic conditions, experiments were carried out with an artificial simulator.[3–5] One set of heat sources consisted of 84 electrical energy supplies (110 V, 125 W). During operations, the strengths of the heat sources were adjusted by using a set of on–off switches. The insolations I_0 were measured and recorded with an Epply laboratory pyranometer. Wind was provided by a fan and the wind velocity V was set at 1.0 m/s (as indicated by a Chicago Cenco anemometer). Temperatures were measured on the outside glass cover and on the absorbing surface at several points with a No. 709 probe from the Yellow Springs Instrument Co., while the ambient temperature ($T_a = 30°C$) was controlled by using an air conditioner and was measured at a position 15 cm above the outside glass cover with a No. 705 probe. In addition, 12 mercury thermometers were employed to measure air temperatures within the heater and also at the inlet (T_i) and outlet (T_o). The temperature of inlet air (T_i) was controlled at 35°C.

Except for the glass cover, all parts of the solar air heater were well insulated thermally to make the energy loss as small as possible. For each heater, an air box with a preheater was used for air distribution and temperature control at the inlet. Air to be heated was supplied steadily by a blower (Redmond Co. Model BL Model 552) and the flow rate was controlled by a transformer, while the flow rate was measured with a No. 3132 Taylor anemometer from Fisher Scientific Co.

Experimental results. At the end of each experimental run, air temperatures in the interior and at the inlet and outlet of the collector, the ambient temperature and the mass-flow rate were measured. It was found that the temperatures of the absorbing plate and bulk fluid are mainly functions of the flow direction. The experimental values of the total collector efficiency were then calculated from the relation:

$$\eta = (\dot{m}C_p/A_c I_o)(T_o - T_i). \tag{25}$$

The results are plotted in Figs. 2 and 3.

Theoretical predictions. The method for theoretical predictions of collector efficiencies was described in previous sections. The following and Table 1 are the experimental conditions and physical properties employed in this study: A_c = BL = 0.42132 m^2, L = 26.5 cm, B = 159 cm; B_1/B = 1/6, 1/5, 1/4, 1/3, 1/2, 2/3, 3/4, 4/5, 5/6 and 1/1 (without a barrier); H = 5.5 cm, $\tau_g = 0.875$, $\alpha_p = 0.95$, $\epsilon_R = 0.94$, $\epsilon_g = 0.94$, $U_b = k_s/l_s \approx 0$, I_0 = 830 and 1100 W/m^2; $T_a = 30°C$, T_i = (35 ± 0.1)°C; V = 1.0 m/s; $\dot{m}$ = 0.0107, 0.0161 and 0.0214 kg/s.

By substituting the specified values into the appropriate equations, theoretical predictions were obtained. The results are also plotted in Figs. 2 and 3.

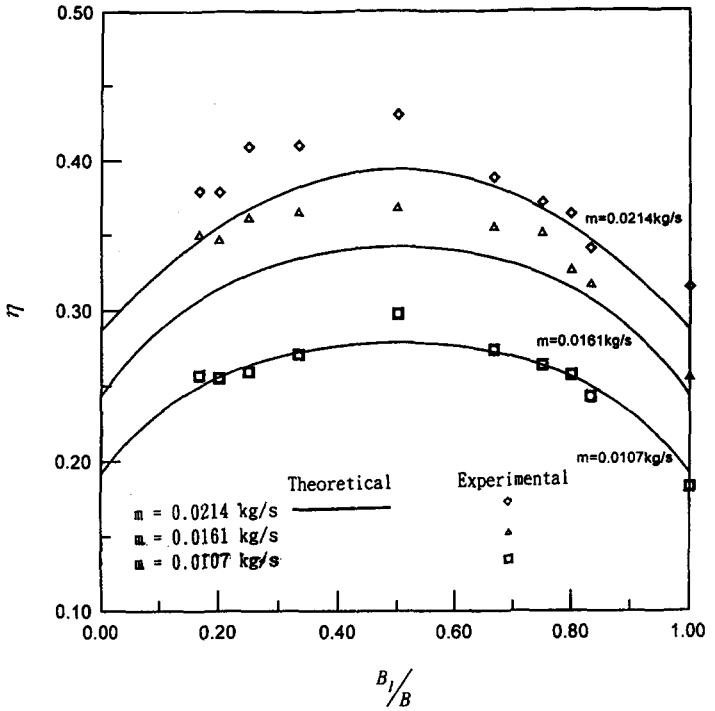

Fig. 2. Effect of barrier location on collector efficiency; $I_0 = 1100\ W/m^2$.

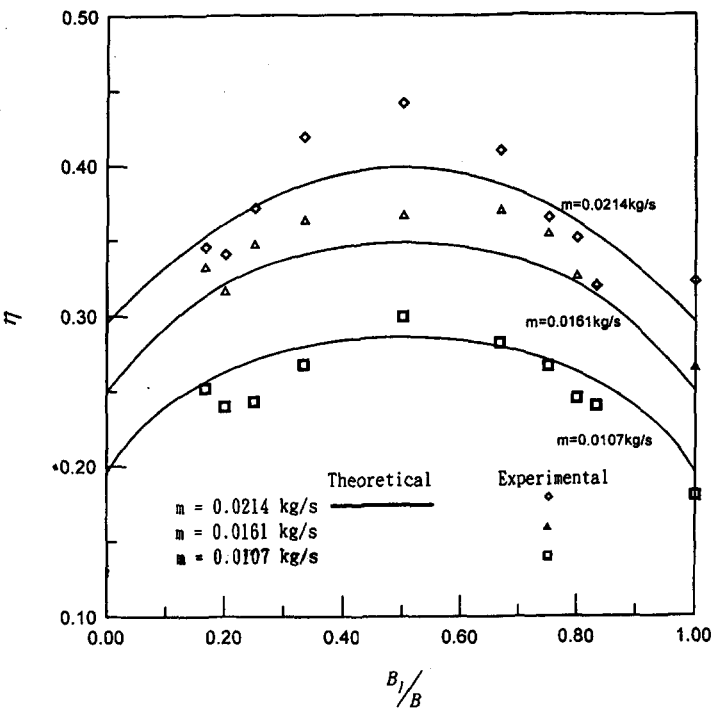

Fig. 3. Effect of barrier location on collector efficiency; $I_0 = 830\ W/m^2$.

DISCUSSION AND CONCLUSIONS

It is seen from Figs. 2 and 3 that the theoretical prediction agree reasonably well with the experimental results. We also found that the improvements in collector efficiency are achieved by placing a parallel barrier on the collector. With a constant collector length L and collector width B (i.e. $A_c = BL$ = constant), the collector efficiency increases when the barrier is placed at the center line of the collector

Table 1. Physical properties of air at 1 atm.

T (°C)	ρ (kg/m³)	C_p (kJ/kg-K)	$\mu \times 10^5$ (kg/m-s)
10.0	1.246	1.0048	1.78
37.8	1.137	1.0048	1.90
65.6	1.043	1.0090	2.03
93.3	0.964	1.0090	2.15

with $B_1/B = 0.5$. When the barrier is placed exactly at $B_1/B = 0.5$, the performance of our collector (L = 26.5 cm, B = 159 cm) is equivalent to that with L = (2 × 26.5) cm and B = (159/2) cm but without a barrier. Therefore, the result of our study confirms previous work[15] in which we indicated that with constant collector area, the collector efficiency increases when the collector aspect ratio (L/B) increases. We therefore believe that the more parallel barriers we place inside the collector with the same distance between any two of them, the higher the collector efficiency that will be obtained because increasing either the aspect ratio or barrier number decreases the cross-sectional area of the air duct and thus increases the velocity of air flow as well as the convective heat-transfer rate from the surface of the absorbing plate to the flowing air.

The improvement in collector efficiency of barrier solar air heaters may be quantified by:

$$I(\text{in}\%) = 100(\eta - \eta_0)/\eta_0, \tag{26}$$

where η_0 denotes the collector efficiency of a solar air heater with the same collector area and configuration but without barrier ($B_1/B = 1$). Tables 2 and 3 show theoretical calculations of improvements in collector efficiency for two flat-plate solar air heaters with the same collector area, each with a parallel barrier. These data show that the optimum barrier location $(B_1/B)_{opt}$ for best collector performance is the center of the collector at $B_1/B = 0.5$, and that the improvement increases with insolation or as the flow rate decreases. Collector efficiencies of heaters with smaller collector aspect ratios are lower than those with larger collector aspect-ratios but the improvement in collector efficiency is greater.

Although the effect of increasing the collector aspect ratio on collector efficiency in a solar air heater is equivalent to increasing the number of parallel-plate barriers in a solar air heater with the same collector area and configuration, heat loss to the ambient from the solar air heater of larger aspect ratio without barriers may be greater than that of a collector with smaller aspect ratio and with barriers. We conclude that placing parallel barriers uniformly on a collector is a desirable and economical procedure for designing and constructing useful solar air heaters.

Table 2. Improvements in collector efficiency for a solar air heater with a parallel barrier placed on the collector (L = 26.5 cm, B = 159 cm).

I_0 (W/m²)	$\dot{m}$ (kg/s)	η_0	I (%)				
			B_1/3=1/2	B_1/B=1/3 or 2/3	B_1/B=1/4 or 3/4	B_1/B=1/5 or 4/5	B_1/B=1/6 or 5/6
1100	0.0107	0.189	45.50	42.32	38.09	34.39	31.21
	0.0161	0.243	39.91	36.62	32.51	28.80	25.92
	0.0214	0.284	35.91	32.74	28.87	25.35	22.88
830	0.0107	0.197	43.65	40.10	36.04	32.48	29.44
	0.0161	0.250	38.40	35.20	31.20	27.60	25.20
	0.0214	0.292	33.90	30.82	27.05	23.97	21.57

Table 3. Improvements in collector efficiency for a solar air heater with a parallel barrier placed on the collector (L = 79.5 cm, B = 53 cm).

I_0	$\dot{m}$	η_0	I (%)				
(W/m²)	(kg/s)		B_1/B=1/2	B_1/B=1/3 or 2/3	B_1/B=1/4 or 3/4	B_1/B=1/5 or 4/5	B_1/B=1/6 or 5/6
1100	0.0107	0.299	32.05	29.27	25.75	22.71	20.53
	0.0161	0.364	26.60	24.13	21.08	18.47	16.61
	0.0214	0.411	22.93	20.74	18.06	15.77	14.17
830	0.0107	0.306	30.54	27.86	24.49	21.58	19.49
	0.0161	0.370	25.29	22.94	20.05	17.56	15.78
	0.0214	0.415	21.90	19.81	17.25	15.06	13.52

REFERENCES

1. M. K. Seluck, in *Solar Air Heaters and Their Applications*, pp. 155–182, A. A. M. Sayigh ed., Academic Press, NY (1977).
2. F. Kreith and J. F. Kreider, *Principles of Solar Engineering*, pp. 203–309, McGraw-Hill, NY (1978).
3. H. M. Yeh and Y. C. Ting, *Appl. Energy* **22**, 145 (1986).
4. H. M. Yeh and Y. C. Ting, *Energy—The International Journal*, **13**, 543 (1988).
5. H. M. Yeh and T. T. Lin, *Energy—The International Journal*, **20**, 1041 (1995).
6. A. Whillier, *Solar Energy Collection and Its Utilization for House Heating*, ScD Thesis, MIT (1953).
7. H. C. Hottel and A. Whillier, *Transactions of the Conference on the Use of Solar Energy*, **2**, Part I, 74, University of Arizona Press, Tucson, AZ (1958).
8. A. Whillier, *Applications of Solar Energy for Heating and Cooling of Buildings*, ASHRAE, NY (1977).
9. R. W. Bliss, *Solar Energy*, **3**(4), 55 (1959).
10. J. A. Duffie and W. A. Beckman, *Solar Engineering of Thermal Processes*, 3rd edn, pp. 238 and 245, Wiley, NY (1980).
11. S. A. Klein, *Solar Energy* **17**, 79 (1979).
12. H. C. Hottel and B. B. Woetz, *Transactions of the American Society of Mechanical Engineers* **64**, 91 (1942).
13. W. M. Kays, *Convective Heat and Mass Transfer*, McGraw-Hill, NY (1996).
14. W. H. McAdams, *Heat Transmission*, 3rd edn, McGraw-Hill, NY (1954).
15. J. A. Duffie and W. A. Beckman, *Solar Engineering of Thermal Processes*, 3rd edn, p. 223, Wiley, NY (1980).

NOMENCLATURE

A_c = surface area of the collector, LB (m^2)
B = collector width (m)
C_p = specific heat of air at constant pressure (kJ kg^{-1} K^{-1})
D_e = equivalent diameter of the conduit (m)
F' = efficiency factor of the solar air heater
F_R = heat-removal factor for the solar air heater
H = height of the air tunnel in the solar collector (m)
h, h_1, h_2 = convective heat-transfer coefficient for fluid flowing over a flat plate (kJ-h^{-1}-m^{-2}-K^{-1})
h_r = radiant heat-transfer coefficient between two parallel plates (kJ-h^{-1}-m^{-2}-K^{-1})
h_w = connective heat-transfer coefficient for air flowing over the outside
Q_u = useful gain of energy carried away by air per unit time (kJ-h^{-1})
Re = Reynolds number
T_a = ambient temperature (K)
$T(z)$ = fluid temperature (K)
T_1, T_2 = T in subcollector 1 or 2 (K)
$T_{1,L}$ = T at the outlet of subcollector 1 or at the inlet of subcollector 2 (K)
T_i, T_0 = T at the inlet and outlet of the solar air heater (K)
$\bar{T}$ = average value of T (K)
T_p, T_R = temperature of the absorbing plate, bottom plate (K)
$\bar{T}_p$ = average value of T_p (K)
U_b = loss coefficient from the surfaces of edges and the bottom of the solar collector to the ambient (kJ-h^{-1}-m^{-2}-K^{-1})
U_L = overall loss coefficient (kJ-h^{-1}-m^{-2}-K^{-1})
U_t = loss coefficient from the top of the

surface of glass cover (kJ-h^{-1}-m^{-2}-K^{-1})
I_0 = incident solar radiation (kJ-m^{-2}-h^{-1})
k,k_s = thermal conductivity of air, insulator (kJ-h^{-1}-m^{-1}-K^{-1})
L = collector length (m)
l_s = thickness of the insulator (m)
$\dot{m}$ = mass-flow rate of air (kg-h^{-1})
$\epsilon_g,\epsilon_p,\epsilon_R$ = emissivity of the glass cover, absorbing plate, bottom plate
ρ = air density (kg-m^{-3})
μ = air viscosity (kg-m^{-1}-h^{-1})
σ = Stefan-Boltzmann constant, 2.04×10^{-7} (kJ-h^{-1}-m^{-2}-K^{-4})
solar collector to the ambient (kJ-h^{-1}-m^{-2}-K^{-1})
v = air velocity in the tunnel (m-h^{-1})
V = wind velocity (m-h^{-1})
z = axial coordinate along the flow direction (m)
α_p = absorptivity of the absorbing plate
τ_g = transmittance of the glass cover
η = collector efficiency, defined by Eq. (25)
η_0 = η obtained in the collector without barrier ($B_1/B = 1$)

Subscript
1,2 = subcollector 1, 2